SYNTHESIS OF NEW CHLOROQUINE DERIVATIVES FOR BIOLOGICAL STUDIES

Abdullah Y. Saad[1], Abdelrahman S. Mayhoub[1,2], Korany A. Ali[3, 4], Mohamed M. Elsebaei[1]*.

[1]Department of Pharmaceutical Organic Chemistry, College of Pharmacy, Al-Azhar University, Cairo, 11884, Egypt

[2]Nanoscience Program, University of Science and Technology, Zewail City of Science and Technology, Giza, Egypt

[3]Center of Excellence, Advanced Material & Nanotechnology Group, National Research Centre,

[4]Applied Organic Chemistry Department, National Research Centre, 12622 Dokki, Giza, Egypt

*Corresponding author: m.elsebaei@azhar.edu.eg

ABSTRACT

This study focused on the development of novel chloroquine derivatives as potential antiviral agents against SARS-CoV-2. By modifying the 7-position of chloroquine using Sonogashira and Buchwald cross-coupling reactions, a series of compounds were synthesized. *In vitro* evaluations identified several derivatives with promising antiviral activity, with compound **9d** exhibiting strong inhibitory effects and a favorable selectivity index. These results suggest that the derivatives provide a promising basis for further optimization and development as antiviral drugs. This work highlights the potential of structural modifications to improve the effectiveness of chloroquine derivatives. Given the ongoing challenges of COVID-19, these novel compounds deserve further investigation to determine their mechanisms of action and therapeutic value. This study provides important insights into antiviral drug development and highlights the need for continued efforts to optimize existing drug scaffolds in the fight against emerging viral threats.

Keywords: *Chloroquine, COVID-19, Sonogashira cross-coupling, Buchwald cross-coupling, Antiviral agent.*

1. Introduction

In December 2019, numerous cases of pneumonia were reported in China (Wang, Wang et al. 2020). Furthermore, it spreads to other neighboring countries. Cases with similar symptoms were reported worldwide in early 2020. Since the start of the pandemic, the global number of COVID-19 cases has surpassed 704 million, with about 7 million deaths reported (Dong, Du *et al*. 2020). A novel virus identified as a new member of the coronavirus family has been named COVID-19. COVID-19 caused a range of physical symptoms. Infected people often suffer from fever, diarrhea, cough, and inflammation in their upper respiratory tract. In addition to this physical challenge, the anxiety and fear associated with the disease could worsen the individual's health (Wang, Horby *et al*. 2020).

In the race to find a solution to COVID-19, researchers worldwide are rushing to develop vaccines and antiviral drugs. Meanwhile, medical institutions are testing existing drugs for other diseases to determine their effectiveness against the coronavirus (Kozlov 2022, Shahin, Mohamed *et al.* 2023). These drugs, including chloroquine, hydroxychloroquine and several others, have shown promising activity in laboratory studies. However, there has been a recent debate about the use of chloroquine to treat COVID-19, even though it is permitted in some countries (Devaux, Rolain *et al*. 2020).

Chloroquine, a well-known weak base with an aromatic quinoline scaffold (El-Gamal, Sherbiny *et al*. 2015), was synthesized by Bayer in 1934 (Sharma, Deep *et al*. 2017). It is rapidly absorbed by the intestines and excreted *via* the kidneys. Chloroquine is known for its potent anti-malarial effects and its use in the treatment of rheumatic diseases.   In addition, it has already been used as an antiviral against SARs-CoV-1. Chloroquine is known to increase the pH of the phagolysosome, thereby impairing the lysosomal enzymes that play a crucial role in viral replication (Schrezenmeier and Dörner 2020). The 4-aminoquinoline scaffold has consistently drawn the attention of researchers, primarily due to its potential for modification to enhance therapeutic efficacy. Previous studies have extensively focused on altering the side chain of position 4 to improve activity against chloroquine-resistant *Plasmodium falciparum* strains beside enhance the safety profile which lead to develop of medicines in the market as hydroxychloroquine and amodiaquine **(Figure-1-A)** (Kucharski, Jaszczak et al. 2022). More recently, after the pandemic, attention has shifted to the basic amine side chain modifications aimed at enhancing antiviral activity **(Figure-1-B)** (Herrmann, Hahn et al. 2022). Building on these findings, our work explores the modification of the 7-position of the 4-aminoquinoline core, a less-studied yet promising site for structural optimization. By targeting this position, we aim to enhance the antiviral properties of chloroquine, providing a novel approach informed by previously reported studies.
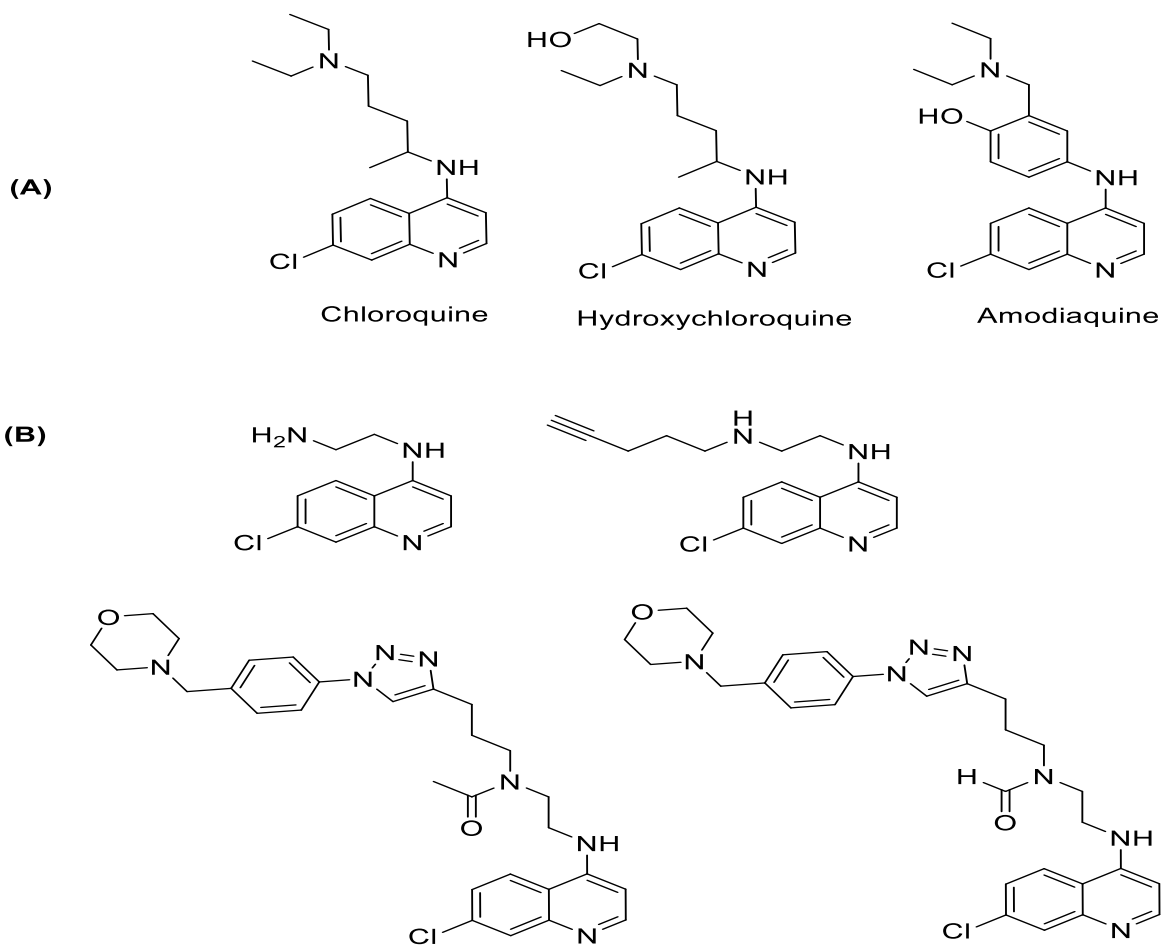
Figure 1: (A): 4-aminoquinoline substructure in market. **(B):** Chloroquine analogues as anti-viral activity.

Here, we want to study new chloroquine analogues to find out their antiviral activity by changing the 7-position on their scaffold. Therefore, we reported the synthesis of bromoquine and iodoquine, which serve as reactive starting materials for derivatization *via* Sonogashira and Buchwald cross-coupling reactions. By exploring the effect of lipophilic and nitrogen-containing substituents on antiviral activity (**Figure-2**).
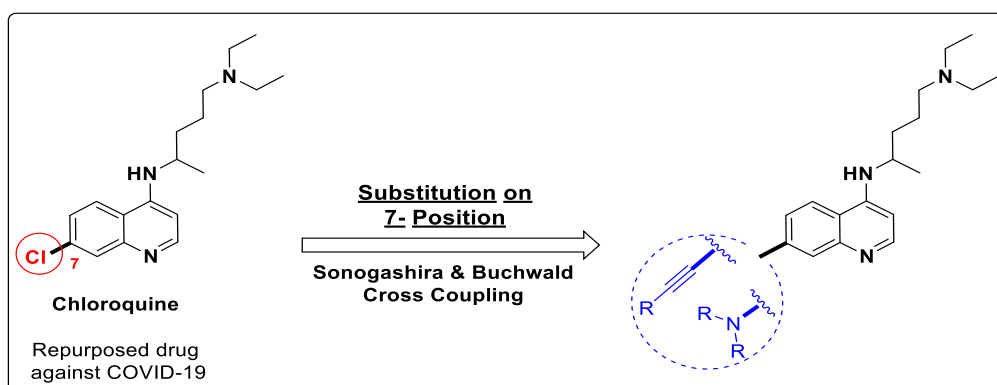

Figure 2: Rational design of this work.

2.   Results and Discussion
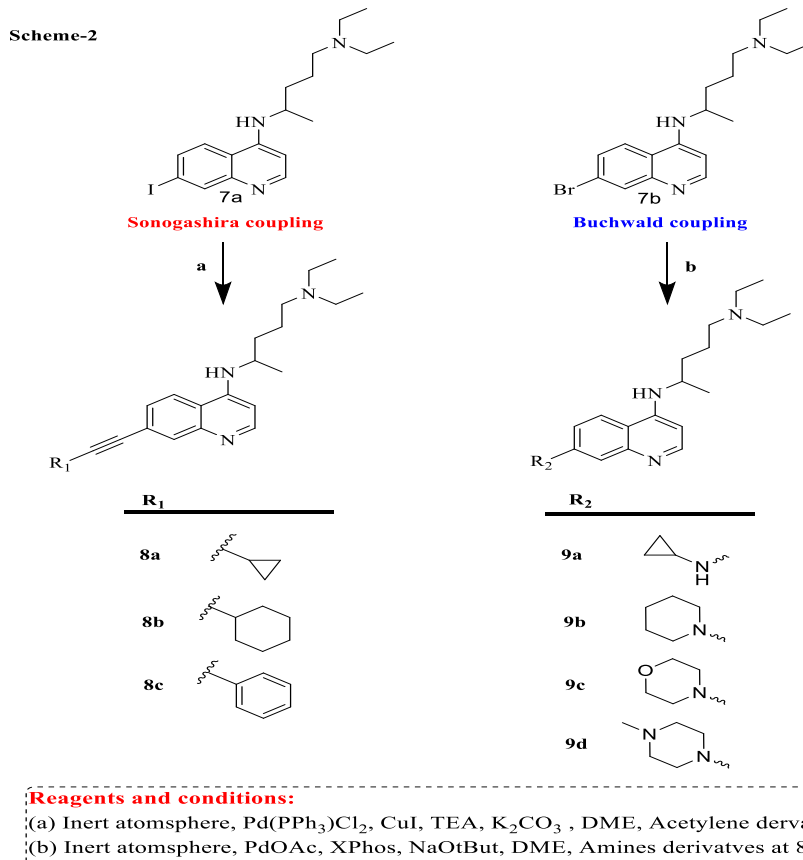## 2.1.   Chemistry

The compound array was produced using a previously established method (Scheme 1) (De, Krogstad et al. 1998). The primary challenge in this work was to establish a synthetic route for the development of 7-iodo and 7-bromo quinolone that are the key intermediate for our compound array, whose differ in reactivity from chloroquine, enabling their susceptibility to coupling reactions. This was achieved by adapting and optimizing a previously reported synthetic pathway. The condensation reaction of *meta*-halogenated aniline **1** with Ethoxymethylenemalonic acid diethyl ester as solvent afforded N-substituted acrylates **2**, and the subsequent thermal cyclization of compound **2** in Ph_2O led to the formation of quinoline scaffold **3**. After that, the basic hydrolysis of compound **3** was conducted using NaOH. Subsequently, thermal decarboxylation in Ph_2O and chlorination with $POCl_3$ gave compound **6** in high yields (De, Krogstad et al. 1998).The amination of the 4-position of compound **6** was carried out using a mixture of TEA together with K_2CO_3 in NMP as solvent to afford compound **7** (Scheme-1) (De, Krogstad et al. 1998, Hwang, Kawasuji et al. 2011).The developed quinoline analogues were produced from the key intermediates **7a** and **7b** via the well-established conditions in our lab for Pd-catalyzed cross coupling reactions (Sonogoshira **8a-c** and Buchwald **9a-d**)(Helal, Sayed et al. 2019, Omara, Hagras et al. 2023, Sayed, Abutaleb et al. 2023). (Scheme-2) (Hammad, Abutaleb et al. 2019) (Mancy, Abutaleb et al. 2019, Hosny, Abutaleb et al. 2020) (Elsebaie, El-Din et al. 2022, El-Din, Elsebaie et al. 2023).

Scheme-1
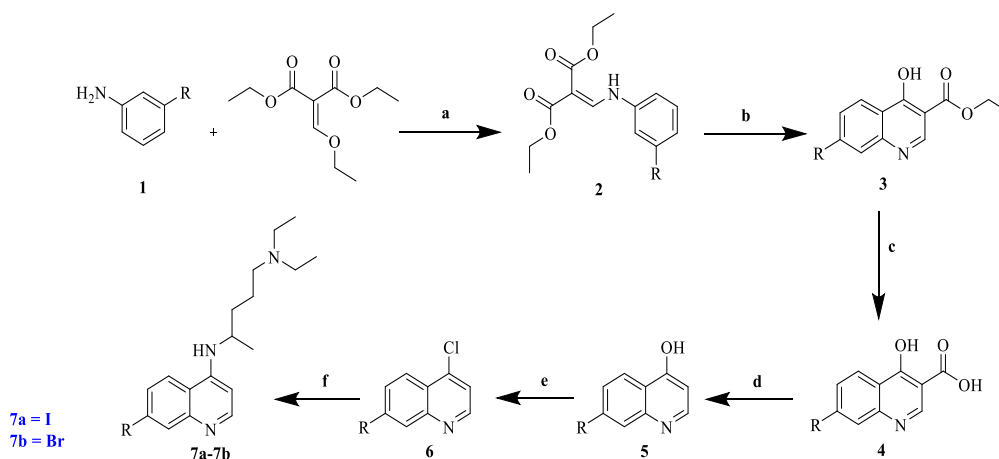
Reagents and conditions:
(**a**) Heat to 90 ºC under N_2 flushing, for 0.5h; (**b**) **2**, added portion wise to PhO_2 at 250 ºC for 12 h;(**c**) 2N aq. NaOH at 150 ºC, then neutralization; (**d**) **4**, added portion wise to PhO_2 at 250 ºC for 6 h; (**e**) $POCl_3$, Reflux for 6 h; (**f**) TEA, K_2CO_3, NMP at 140 ºC.

Scheme-2

Reagents and conditions:
(a) Inert atomsphere, $Pd(PPh_3)Cl_2$, CuI, TEA, K_2CO_3 , DME, Acetylene dervatives at 100 ºC.
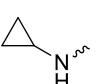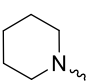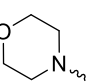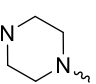(b) Inert atomsphere, PdOAc, XPhos, NaOtBut, DME, Amines derivatves at 80 ºC.
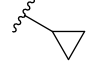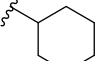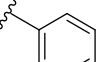
2.2. Biological Evaluation

2.2.1. Antiviral studies

The effectiveness of new compounds against the SARS-CoV-2 virus was evaluated with a standard laboratory method using the VERO-E6 technique (normal kidney cells of Clorocebus aethiops) (Wyman, Girgis et al. 2022, Shahin, Mohamed et al. 2023). Some of these compounds showed promising antiviral activity. For example, compound **8a** with the cyclopropylacetylene moiety showed the best effective inhibitory properties (IC_{50} = 10.7 µM, CC_{50} = 73.89 µM, and SI = 6.9). Replacing cyclopropyl with cyclohexyl **8b** or phenyl **8c** deteriorated the safety profile of these compounds (CC_{50} = 12 and 4 µM, respectively). The transition to nitrogen-containing derivatives (**9a-d**) showed a fluctuation in activity. Regarding primary amine, the cyclopropylamine derivative **9a** exhibited an excellent safety profile (CC_{50} =712.7 µM), but unfortunately, the antiviral activity disappeared (IC_{50} = 204 µM). On the other hand, secondary amines (**9b-9d**) provided a reasonable balance between antiviral activity and cytotoxicity. Compounds **9b** and **9c** piperidine and morpholine derivatives showed almost similar activity and cytotoxicity (IC_{50}s = 43.5 and 44.6 µM, CC_{50s} = 314 and 324.7 µM, and SI = 7.2 and 7.26). While the *N*-methylpi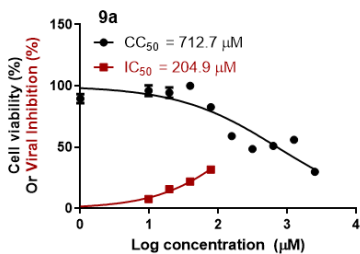prazine derivative **9d** showed sufficient inhibitory effect with a plausible selectivity index (IC_{50} = 43 µM, CC_{50} = 633 µM, and SI = 14.7) (**Table-1** and **Figure 3**).

Table 1: Antiviral activity of chloroquine derivatives

R	Code	IC50	CC50	SI
cyclopropyl	8a	10.7	73.98	6.9
cyclohexyl	8b	ND	12	ND
phenyl	8c	ND	4.419	ND
cyclopropyl-NH	9a	204.9	712.7	3.47
piperidinyl	9b	43.57	314.6	7.22
morpholinyl	9c	44.67	324.7	7.26
N-methylpiperazinyl	9d	43.15	633.8	14.7
Chloroquine Standard		8.04	199.4	24.8

ND: Not determined
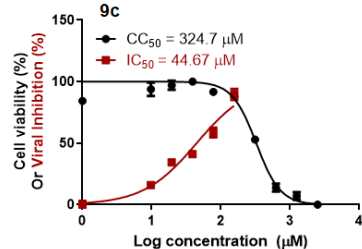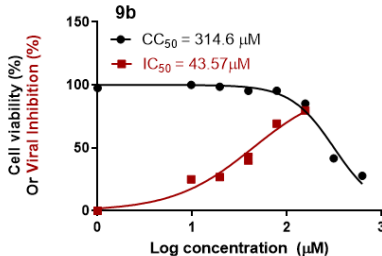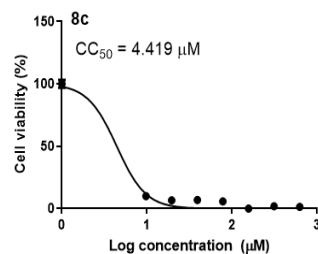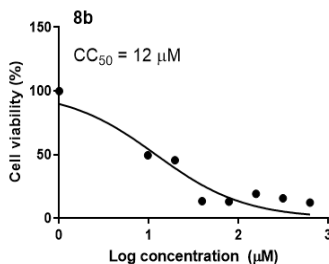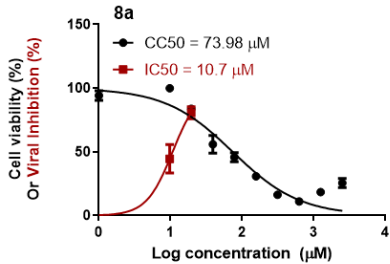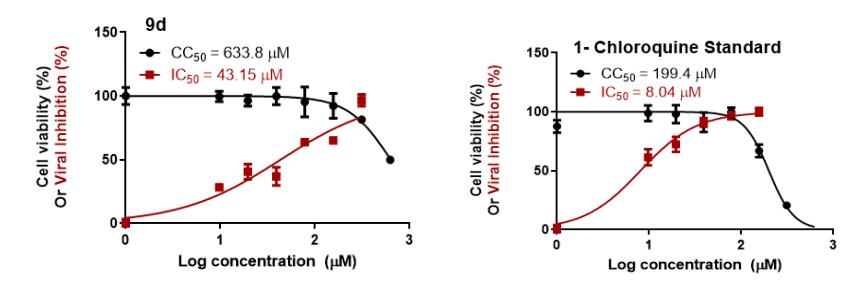
Figure 3. Dose–response curves for the chloroquine derivatives as anti-SARS-CoV-2

2.2.2   In silico studies

2.2.2.1.   **Computational analysis:** *In silico* **prediction of physicochemical properties, pharmacokinetics, and drug-likeness profile**

The process of predicting pharmacokinetics is considered an important topic in drug development. This is because it helps drug developers to either modify the guideline or pass it on to another candidate. In the last two decades, some online tools and programs have been developed to predict absorption, distribution, metabolism and excretion (ADME). In this study, the ADME properties of the two most active candidates in our library were calculated and the result is summarized in Tables 2-4. Three programs were used to study the ADME, similarity and physiochemical properties of the top three candidates: PreAdME, SwissAdme, and Molsoft.

Table 2: Physiochemical properties prediction through SwissADME (Jia, Li et al. 2020)

Code	tPSA[a]	H-bond Donor	H-bond acceptor	NORTB[b]	MW[c]	Log P
9c	40.63	1	3	9	370.53	**4.11**
9d	34.64	1	3	9	383.57	**4,3**
Chloroquine	**28.16**	**1**	**2**	**8**	**319.87**	**3.95**

a- Topological Polar Surface Area
b- Num. rotatable bonds
c- Molecular weight

Table 3:   Predicting drug-likeness using Molosoft (Amin, El-Saadi et al. 2021) SwissADME.

Code	Solubility (mg/L)	Drug likeness model score	Lipinski's rule violation	Bioavailability score
9c	1.3	0.29	0	**0.55**
9d	1.4	0.75	0	**0.55**
Chloroquine	**3.86**	**0.48**	**0**	**0.55**

Understanding the physicochemical properties of therapeutic compounds is crucial for predicting their pharmacokinetic behavior and potential efficacy. **Table 2** and **3** shows the predictions of key physicochemical properties for chloroquine and its derivatives **9c** and **9d**, as assessed through SwissADME (Jia et al., 2020). These properties include topological polar surface area (tPSA), number of hydrogen bond donors and acceptors, number of rotatable bonds (NROT), molecular weight (MW), and log P values, all of which play significant roles in a compound's solubility, permeability, and overall bioavailability.

Chloroquine is characterized by a lower tPSA and lower molecular weight, which contribute to its favorable solubility and permeability. In contrast, derivatives **9c** and **9d** exhibit higher logP values and differences in hydrogen bonding properties, suggesting increased lipophilicity. Specifically, **9d** with the highest molecular weight and logP, has an increased membrane permeability potential; However, solubility limitations can also occur. In brief, Chloroquine has the lowest molecular weight, tPSA and LogP, which could make it more bioavailable and soluble while maintaining good permeability. Derivatives **9c** and **9d** are more lipophilic (higher LogP) and have more hydrogen bond acceptors, which may impact their binding affinity with biological targets **9d** with the highest molecular weight and LogP, is the most lipophilic of the three compounds in the tables and although it may have better membrane permeability, it could have solubility challenges compared to chloroquine (Caron, Ermondi et al. 2009, Helal, Hussien et al. 2022, O'Donovan, De Fusco et al. 2023, Atwa, Hagras et al. 2024, Awaji, El Zaloa et al. 2024, Elsebaei, Ezzat et al. 2024, Abuelkhir, Nagy et al. 2025).

Lipiniski rule (Awaji, El Zaloa *et al.* 2024): states that the oral drug have no violation of the following criteria: no more than 5 HBD and no more than 10 HBA, molecular weight less than 500 Daltons and logP including the value 5. Using SwissADME and Molsoft, our compounds met Lipinski's rules for drug-likeness; For this reason, we believe that they have good absorption. The solubility of the drug is a crucial factor in determining the rate of dissolution that enables oral bioavailability; therefor, solubility of the drug is tested, which improves when the solubility values are less than 10 mg/L. Since our compounds show values from 1-5 mg/L, then, they are poor soluble in water (Helal, Hussien *et al*. 2022). Chloroquine remains a benchmark due to its established pharmacokinetic characteristics, including favorable blood-brain barrier penetration (BBB) and good intestinal absorption (CACO-2). In comparison, the derivatives **9c** and **9d** have different profiles, particularly in terms of their human intestinal absorption (HIA) and their permeability to Madin-Darby canine kidney cells (MDCK). Notably, **9d** exhibits increased permeability across biological membranes but may have problems with solubility, which is crucial for its bioavailability. The data indicate that while **9c** and **9d** possess properties that may improve therapeutic outcomes, careful consideration of their pharmacokinetic properties, including their interactions with cytochrome P450 2D6 (CYP2D6), is vital for predicting their behavior *in vivo*.

Table 4: Pharmacokinetics prediction through pre-ADME

Pharmacokinetics

Code	[a]BBB	[b]CACO-2 (x10^6 cm/s)	[c]HIA (%)	[d]MDCK (nm/s)	[e]PPB(%)	[f]CYP2D6
9c	0.96	28.31	96.49	24.96	69.71	*substrate*
9d	2.44	22.19	96.87	2.19	21.60	*substrate*
Chloroquine	7.73	56.61	98.05	0.29	92.53	*substrate*

[a]BBB: blood-brain barrier penetration.
[b]CACO-2: permeability through cells derived from human colon adenocarcinoma.
[c]HIA: percentage of human intestinal absorption.
[d]MDCK: permeability through Madin-Darby canine kidney cells.
[e]PPB: plasma protein binding.
[f]CYP2D6: cytochrome P450 2D6.

2.2. Prediction of Toxicity

Predicting the toxicity of a compound is a critical step in the development of new drug candidates, making *in silico* toxicity studies a faster and cheaper procedure than *in vivo* animal toxicity testing or *in vitro* testing in cell lines. It also helps significantly reduce the number of animals used in experimental assays (Banerjee, Eckert *et al.* 2018). There are several online programs that access toxicities that are used *in silico* models to predict mean lethal dose, carcinogenicity، mutagenicity, and more.

The Pro-Tox II web server (Banerjee, Eckert *et al.* 2018) predicts the mean lethal dose (LD$_{50}$) in rodents. According to this program, all compounds can be classified into six GHS (Globally Harmonized System of Classification and Labeling of Chemicals) Categories (Angeli, Petrou *et al.* 2023) according to their toxicity and LD$_{50}$ value.

Toxicity classes are defined according to the globally harmonized system of classification of labeling of chemicals (GHS). LD$_{50}$ values are given in [mg/kg]:

■ Class I: fatal if swallowed (LD$_{50}$ ≤ 5)

■ Class II: fatal if swallowed (5 < LD$_{50}$ ≤ 50)

■ Class III: toxic if swallowed (50 < LD$_{50}$ ≤ 300)

■ Class IV: harmful if swallowed (300 < LD$_{50}$ ≤ 2000)

■ Class V: may be harmful if swallowed (2000 < LD$_{50}$ ≤ 5000)

■ Class VI: non-toxic (LD$_{50}$ > 5000)

Toxicity assessment is an important part of the development of therapeutic agents as it directly impacts their safety profile and potential clinical applications. **Table 5** summarizes the predicted toxicity for chloroquine and the new derivatives **9c** and **9d**, focusing on key parameters such as LD_{50} values and classifications for hepatotoxicity, carcinogenicity, mutagenicity and cytotoxicity.

The data suggests that both derivatives have promising safety profiles, with **9c** showing a higher predicted LD_{50} (1040 mg/kg) and being classified in toxicity class IV, suggesting a lower risk of acute toxicity. Conversely, at **9d**, although still in a relatively safe range with a predicted LD_{50} of 750 mg/kg, there are active concerns for mutagenicity that warrant further investigation. Although chloroquine is effective, it has higher toxicity in certain categories, particularly hepatotoxicity and mutagenicity.

These results highlight the potential of derivatives **9c** and **9d** as safer alternatives to chloroquine, particularly in terms of hepatotoxicity and overall toxicity class. However, the active mutagenicity observed with **9d** highlights the need for thorough preclinical evaluations to ensure patient safety.

Table 5: Prediction of toxicity

No	Predicted LD_{50} (mg/kg)	Predicted Toxicity Class	Hepatotoxicity	Carcinogenicity	Mutagenicity	Cytotoxicity
9c	1040	IV	Inactive (0.84)	Inactive (0.60)	active (0.58)	Inactive (0.71)
9d	750	IV	Inactive (0.84)	Inactive (0.70)	active (0.63)	Inactive (0.71)
chloroquine	750	IV	Inactive (0.90)	Inactive (0.66)	active (0.94)	Inactive (0.93)

3. Conclusion:

In this study, we successfully synthesized and evaluated a series of novel chloroquine derivatives as potential antiviral agents against SARS-CoV-2. By modifying the 7-position of the chloroquine scaffold, we developed compounds that exhibited promising antiviral activity. Notably, derivatives containing cyclopropylacetylene, *N*-methylpiprazine and morpholine moieties demonstrated significant inhibition of SARS-CoV-2 replication while maintaining acceptable safety profiles. Among them, compound **9d** emerged as an outstanding candidate, showcasing excellent inhibitory properties with a favorable selectivity index.

Our results highlight the importance of structural modifications in enhancing the antiviral efficacy of chloroquine derivatives. The incorporation of lipophilic and nitrogen-containing substituents at the 7-position not only improved antiviral activity but also suggested the potential for better pharmacokinetic properties. *In silico* studies also confirmed the favorable drug-likeness and pharmacokinetic profiles of the synthesized compounds, indicating their potential for development as therapeutic agents.

Despite the encouraging results, further optimization and extensive preclinical evaluations are required to improve the efficacy, selectivity and overall safety of these derivatives. Future research should focus on understanding the mechanisms of action and exploring combination therapies to maximize therapeutic outcomes against COVID-19.

4. Experimental
4.1. Chemistry

General. All biologically tested compounds have purity of 98% or greater. ^{1}H NMR spectra were performed at 400 MHz and ^{13}CNMR spectra were determined at 100 MHz in deuterated dimethyl sulfoxide (DMSO-*d6*) on a Varian Mercury VX-400 NMR spectrometer. Chemical shifts are measured in parts per million (ppm) on the delta (δ) scale. The chemical shifts were calibrated relative to those of the solvents. Column chromatography was performed on 230-400 mesh silica. The reaction progress was monitored using Merck silica gel IB2-F plates (0.25 mm thickness). Melting points were determined using capillary tubes with a Stuart SMP30 apparatus and are uncorrected. All yields reported refer to isolated yields. Compound (**7**) was prepared as reported (Hwang, Kawasuji et al. 2011, Elsebaei, Mohammad et al. 2018, Elsebaei, Abutaleb et al. 2019, Elsebaei, Mohammad et al. 2019).

N^4-(7-(Alkylethynyl)quinolin-4-yl)-N^1,N^1-diethylpentane-1,4-diamine (8a-c).

General procedure: to DMF (7 mL) and triethylamine (3 mL) in a sealed 75-mL tube compound **7** (100 mg, 312 mmol), dichlorobis (triphenylphosphine) palladium(II) (21 mg, 10 mol%), copper(I) Iodide (12 mg, 20 mol%) and potassium carbonate (90 mg, 2 equiv.). After the reaction mixture was purged with dry nitrogen gas for 15 minutes, appropriate acetylene derivatives (2 equiv.) were added. The sealed tube was then heated and stirred at 100 °C for 24 hours and monitored using thin-layer chromatography (TLC). After the reaction was completed, the reaction mixture was poured onto water, then extracted with ethyl acetate (3 × 15 mL) then dried over MgSO$_4$, the organic materials were then concentrated under reduced pressure. The raw materials were purified by silica gel flash column chromatography using DCM-MeOH (9:1) as a yellowish viscous oil.

N^4-(7-(Cyclopropylethynyl)quinolin-4-yl)-N^1,N^1-diethylpentane-1,4-diamine (8a). Brown oil (71 mg, 59.2 %); ^{1}H NMR (DMSO-*d6*) δ: 8.32 (d, J = 8.2 Hz, 1H), 8.23 (d, J = 8.1 Hz, 1H), 7.67 (s, 1H), 7.30 (d, J = 6.5 Hz, 1H), 6.76 (brs, 1H), 6.43 (d, J = 6.4 Hz, 1H), 3.70-3.66 (m, 1H), 2.37-2.31 (m, 6H), 1.66-1.45 (m, 5H), 1.19 (d, J = 6.7 Hz, 3H), 0.87-0.74 (m, 10H); ^{13}C NMR (DMSO-*d6*) δ: 153.7, 149.4, 148.9, 130.4, 125.2, 120.4, 117.5, 116.1, 107.0, 89.9, 84.2, 53.7, 47.6, 33.4, 25.0, 16.7, 12.6, 10.5, 0.2; MS (*m/z*); 349.5 (M+, 100.00%).

N^4-(7-(Cyclohexylethynyl)quinolin-4-yl)-N^1,N^1-diethylpentane-1,4-diamine (8b). Brown oil (61 mg, 54.2 %); ^{1}H NMR (DMSO-*d6*) δ: 8.56 (d, J = 8.2 Hz, 1H), 8.01 (d, J = 8.1 Hz, 1H), 7.69 (s, 1H), 7.56 (d, J = 6.5 Hz, 1H), 6.77 (brs, 1H), 6.45 (d, J = 6.4 Hz, 1H), 3.35 -3.29 (m, 1H), 2.37-2.31 (m, 6H), 1.66-1.45 (m, 11H), 1.02-0.74 (m, 13H); ^{13}C NMR (DMSO-*d6*) δ: 153.5, 149.3, 148.7, 130.1, 125.3, 120.6, 117.1, 116.3, 107.1, 85.7, 81.4, 53.2, 47.4, 46.9, 33.1, 29.1, 28.7, 25.3, 24.7, 16.2, 12.6; MS (*m/z*); 391.6 (M+, 100.00%).

N^1,N^1-Diethyl-N^4-(7-(phenylethynyl)quinolin-4-yl)pentane-1,4-diamine (8c). Yellow oil (57 mg, 40.1%); ^{1}H NMR (DMSO-*d6*) δ: 8.37 (d, J = 8.2 Hz, 1H), 8.33 (d, J = 8.1 Hz, 1H), 7.88 (s, 1H), 7.60-7.41 (m, 6H), 6.84 (d, J = 6.4 Hz, 1H), 6.49 (d, J = 6.4 Hz, 1H), 3.72-3.67 (m, 1H), 2.40-2.31 (m, 4H), 1.68-1.43 (m, 6H), 1.21 (d, J = 6.4 Hz, 3H), 0.88 (t, J = 6.7 Hz, 6H); ^{13}C NMR (DMSO-*d6*) δ: 153.8, 149.8, 148.3, 130.3, 129.1, 128.4, 128.1, 125.3, 122.5, 120.1,

117.7, 116.0, 107.2, 91.2, 89.4, 53.6, 47.2, 33.4, 25.3, 16.1, 12.5; MS (*m/z*); 385.5 (M+, 100.00%).

N^7- Alkyl-N^4-(5-(diethylamino)pentan-2-yl)quinoline-4-yl)-4,7-diamine (9a-d).

General procedure: to DME (10 mL) in a 75-mL sealed tube compound **7** (100 mg, 1 mmol), palladium acetate (28 mg, 10 mol%), 2-dicyclohexylphosphino-2',4',6'-triisopropylbiphenyl (X-phos) (60 mg, 15 mol%) and potassium *tert*-butoxide (120 mg, 2.5 equiv.). After the reaction mixture was purged with dry nitrogen gas for 15 min at 70 °C, appropriate *primary* amines (5 equiv.) were added. The sealed tube was then heated and stirred at 100 °C for 24 hours and monitored by thin-layer chromatography (TLC). After completion of the reaction, the reaction mixture was poured on water then extracted with ethyl acetate (3 × 15 mL) then dried over MgSO$_4$, the organic materials were then concentrated under reduced pressure. The crude materials were purified *via* silica gel flash column chromatography using DCM-MeOH (9:1) as yellowish viscous oil.

N^7- Cyclopropyl-N^4-(5-(diethylamino)pentan-2-yl)quinoline-4,7-diamine (9a). Brown oil (61 mg, 58.2 %); ^{1}H NMR (DMSO-*d6*) δ: 8.29 (s, 1H), 8.11 (d, *J* = 8.2 Hz, 1H), 7.68 (d, *J* = 8.1 Hz, 1H), 6.80 (d, *J* = 6.5 Hz, 1H), 6.68 (s, 1H), 6.40 (d, *J* = 6.4 Hz, 1H), 6.08 (brs, 1H), 3.70-3.66 (m, 1H), 2.71-2.51 (m, 6H), 1.67-1.43 (m, 5H), 1.18 (d, *J* = 6.7 Hz, 3H), 0.87-0.74 (m, 10H); ^{13}C NMR (DMSO-*d6*) δ: 153.1, 149.5, 148.6, 139.7, 125.1, 119.1, 117.8, 116.2, 107.2, 53.8, 47.5, 47.1, 33.3, 25.1, 23.3, 16.7, 12.9, 6.2; MS (*m/z*); 340.5 (M+, 100.00%).

N^1, N^1-Diethyl-N^4-(7-(piperidin-1-yl)quinolin-4-yl)pentane-1,4-diamine (9b). Brown oil (51 mg, 48.2 %); ^{1}H NMR (DMSO-*d6*) δ: 8.18 (d, *J* = 8.2 Hz, 1H), 7.67 (d, *J* = 8.1 Hz, 1H), 7.26 (d, *J* = 6.5 Hz, 1H), 6.93 (s, 1H), 6.63 (brs, 1H), 6.40 (d, *J* = 6.4 Hz, 1H), 3.76-3.69 (m, 1H), 2.37-2.31 (m, 6H), 1.66-1.45 (m, 11H), 1.02-0.74 (m, 12H); ^{13}C NMR (DMSO-*d6*) δ: 152.9, 151.8, 148.8, 147.9, 125.2, 117.6, 116.8, 107.7, 52.6, 49.8, 47.3, 33.5, 25.5, 25.1, 16.7, 12.9; MS (*m/z*); 368.5 (M+, 100.00%).

N^1, N^1-Diethyl-N^4-(7-morpholinoquinolin-4-yl)pentane-1,4-diamine (9c). Brown oil (64 mg, 58.2 %); ^{1}H NMR (DMSO-*d6*) δ: 8.19 (d, *J* = 8.2 Hz, 1H), 8.11 (d, *J* = 8.1 Hz, 1H), 7.20 (d, *J* = 6.5 Hz, 1H), 6.98 (s, 1H), 6.84 (brs, 1H), 6.57 (d, *J* = 6.4 Hz, 1H), 3.74-3.65 (m, 1H), 2.37-2.31 (m, 6H), 1.66-1.45 (m, 10H), 1.02-0.74 (m, 12H); ^{13}C NMR (DMSO-*d6*) δ: 152.9, 151.8, 148.8, 147.9, 125.2, 117.6, 116.8, 107.7, 52.6, 49.8, 47.3, 33.5, 25.5, 25.1, 12.9; MS (*m/z*); 370.5 (M+, 100.00%).

N^1, N^1-Diethyl-N^4-(7-(4-methylpiperazin-1-yl)quinolin-4-yl)pentane-1,4-diamine (9d). Brown oil (54 mg, 51.2 %); ^{1}H NMR (DMSO-*d6*) δ: 8.32 (d, *J* = 8.2 Hz, 1H), 8.24 (d, *J* = 8.1 Hz, 1H), 7.61 (s, 1H), 7.31 (d, *J* = 6.5 Hz, 1H), 7.01 (brs, 1H), 6.78 (d, *J* = 6.4 Hz, 1H), 3.74-3.65 (m, 1H), 2.37-2.31 (m, 6H), 1.66-1.45 (m, 10H), 1.02-0.74 (m, 14H); ^{13}C NMR (DMSO-*d6*) δ: 153.5, 152.2, 148.8, 147.9, 125.2, 117.6, 116.8, 107.7, 52.6, 49.8, 47.3, 33.5, 25.5, 25.1, 17.2, 12.9; MS (*m/z*); 383.5 (M+, 100.00%).

4.2. *In vitro* bioassay

Cells and viruses

Vero-E6 cells were cultured in Dulbecco's modified Eagle's medium (DMEM) (Lonza, Basel, Switzerland) containing fetal bovine serum (10%) (Lonza), and an antibiotic antimycotic mixture (1%) (Lonza). The cells were incubated at 37 °C in a humidified atmosphere of 5%

CO2. The MERS-CoV isolates (NRCE-HKU270 (Accession Number: KJ477103.2)) were propagated in VERO-E6 cells. The virus was titrated using plaque titration assay as previously described (Mostafa et al. 2020).

Determination of the half-maximal cytotoxic concentration (CC_{50})

To assess the half-maximal cytotoxic concentration (CC_{50}), stock solutions of the synthetic compounds were prepared in 10% DMSO in D_2O and further diluted to the working solutions with DMEM. The cytotoxic activity of the extracts was tested in Vero-E6 cells using the crystal violet assay as previously by Feoktistova *et al* described (2016) and Al-Rabia *et al* (2021) with minor modifications. Cells were seeded in 96 well-plates (100 µl/well at a density of 3×105 cells/ml) and incubated for 24 h at 37 °C in 5% CO_2. After 24 h, cells were treated with various concentrations of the synthetic compounds in triplicates. Seventy-two hours later, the media supernatant was discarded, and cell monolayers were fixed with 10% formaldehyde for 1 h at room temperature (RT). The fixed monolayers are then dried and stained with 50 µl of 0.1% crystal violet for 20 min on bench rocker at RT. The monolayers are then washed, dried and the crystal violet dye in each well is then dissolved with 200 µl methanol for 20 min on bench rocker at RT. Absorbance of crystal violet solutions is measured at λmax 570 nm as a reference wavelength using a BMG LABTECH®- FLUOstar Omega microplate reader in Ortenberg, Germany.

Determination of inhibitory concentration 50 (IC_{50})

The IC_{50} values for synthetic compounds were determined as previously described (Mostafa *et al*. 2020), with minor modifications. Briefly, in 96-well tissue culture plates, 2.4 × 104 Vero-E6 cells were distributed in each well and incubated overnight at a humidified incubator at 37 °C under 5% CO_2 conditions. The cell monolayers were then washed once with 1x PBS. An aliquot of the MERS CoV virus containing 100 $TCID_{50}$ was incubated with serial diluted concentrations of the tested extracts and kept at 37 °C for 1 h. The Vero-E6 cells were treated with virus/compounds mix and co-incubated at 37 °C in a total volume of 200 µl per well. Untreated cells infected with virus represent virus control, however cells that are not treated and not infected are cell control. Following incubation at 37 °C in 5% CO_2 incubator for 72 h, the cells were fixed with 100 µl of 10% formaldehyde for 20 min and stained with 0.5% crystal violet in distilled water for 15 min at RT. The crystal violet dye was then dissolved using 100 µl absolute methanol per well and the optical density of the color is measured at 570 nm using a BMG LABTECH®- FLUOstar Omega microplate reader in Ortenberg, Germany.

Statistical analysis of data

Statistical analyses of all experiments were performed in three biological repeats. Using GraphPad Prism 5.01 software, statistical tests and graphical data presentation were carried out. Data are presented as the average of the means. The CC_{50} and IC_{50} curves represent the nonlinear fit of "Normalize" of "Transform" of the obtained data, their values were calculated using GraphPad prism as "best fit value".

References

Abuelkhir, A. A., Y. I. Nagy, T. Gamal, A. M. Abdelhalim, A. S. Attia, A. S. Mayhoub and M. M. Elsebaie (2025). "Small Molecule Alkynyl-Phenylaminoguanidines: A New Weapon Against Multi-Drug Resistant Bacteria." ChemistrySelect **10**(4): e202404320.

Amin, N. H., M. T. El-Saadi, A. A. Ibrahim and H. M. Abdel-Rahman (2021). "Design, synthesis and mechanistic study of new 1,2,4-triazole derivatives as antimicrobial agents." Bioorganic Chemistry **111**: 104841.

Angeli, A., A. Petrou, V. Kartsev, B. Lichitsky, A. Komogortsev, C. Capasso, A. Geronikaki and C. T. Supuran (2023). "Synthesis, Biological and In Silico Studies of Griseofulvin and Usnic Acid Sulfonamide Derivatives as Fungal, Bacterial and Human Carbonic Anhydrase Inhibitors." International Journal of Molecular Sciences **24**(3): 2802.

Atwa, S. S., M. Hagras, A. S. Mayhoub and M. Elsebaei (2024). "SYNTHESIS OF SOME NEW AZOLE DERIVATIVES AS ANTIBACTERIAL AGENTS." Al-Azhar Journal of Pharmaceutical Sciences **69**(1): 108-129.

Awaji, A. A., W. A. Z. El Zaloa, M. A. Seleem, M. Alswah, M. M. Elsebaei, A. H. Bayoumi, A. M. El-Morsy, M. Y. Alfaifi, A. A. Shati and S. E. I. Elbehairi (2024). "N-and s-substituted Pyrazolopyrimidines: A promising new class of potent c-Src kinase inhibitors with prominent antitumor activity." Bioorganic chemistry **145**: 107228.

Banerjee, P., A. O. Eckert, A. K. Schrey and R. Preissner (2018). "ProTox-II: a webserver for the prediction of toxicity of chemicals." Nucleic acids research **46**(W1): W257-W263.

Caron, G., G. Ermondi, M. B. Gariboldi, E. Monti, E. Gabano, M. Ravera and D. Osella (2009). "The Relevance of Polar Surface Area (PSA) in Rationalizing Biological Properties of Several cis-Diamminemalonatoplatinum (II) Derivatives." ChemMedChem: Chemistry Enabling Drug Discovery **4**(10): 1677-1685.

Devaux, C. A., J.-M. Rolain, P. Colson and D. Raoult (2020). "New insights on the antiviral effects of chloroquine against coronavirus: what to expect for COVID-19?" International journal of antimicrobial agents **55**(5): 105938.

Dong, E., H. Du and L. Gardner (2020). "An interactive web-based dashboard to track COVID-19 in real time." The Lancet infectious diseases **20**(5): 533-534.

El-Din, H. T. N., M. M. Elsebaie, N. S. Abutaleb, A. M. Kotb, A. S. Attia, M. N. Seleem and A. S. Mayhoub (2023). "Expanding the structure–activity relationships of alkynyl diphenylurea scaffold as promising antibacterial agents." RSC Medicinal Chemistry **14**(2): 367-377.

El-Gamal, K., F. Sherbiny, A. El-Morsi, H. Abu-El-khair, I. Eissa and M. El-Sebaei (2015). "Design, synthesis and antimicrobial evaluation of some novel quinoline derivatives." Pharm Pharmacol Int J **2**(5): 165-177.

Elsebaei, M. M., N. S. Abutaleb, A. A. Mahgoub, D. Li, M. Hagras, H. Mohammad, M. N. Seleem and A. S. Mayhoub (2019). "Phenylthiazoles with nitrogenous side chain: an approach to overcome molecular obesity." European Journal of Medicinal Chemistry **182**: 111593.

Elsebaei, M. M., H. G. Ezzat, A. M. Helal, M. H. El-Shershaby, M. S. Abdulrahman, M. Alsedawy, A. K. Aljohani, M. Almaghrabi, M. Alsulaimany and B. Almohaywi (2024). "Rational design and synthesis of novel phenyltriazole derivatives targeting MRSA cell wall biosynthesis." RSC advances **14**(54): 39977-39994.

Elsebaei, M. M., H. Mohammad, M. Abouf, N. S. Abutaleb, Y. A. Hegazy, A. Ghiaty, L. Chen, J. Zhang, S. R. Malwal and E. Oldfield (2018). "Alkynyl-containing phenylthiazoles: Systemically active antibacterial agents effective

against methicillin-resistant Staphylococcus aureus (MRSA)." European journal of medicinal chemistry **148**: 195-209.

Elsebaei, M. M., H. Mohammad, A. Samir, N. S. Abutaleb, A. B. Norvil, A. R. Michie, M. M. Moustafa, H. Samy, H. Gowher and M. N. Seleem (2019). "Lipophilic efficient phenylthiazoles with potent undecaprenyl pyrophosphatase inhibitory activity." European journal of medicinal chemistry **175**: 49-62.

Elsebaie, M. M., H. T. N. El-Din, N. S. Abutaleb, A. A. Abuelkhir, H.-W. Liang, A. S. Attia, M. N. Seleem and A. S. Mayhoub (2022). "Exploring the structure-activity relationships of diphenylurea as an antibacterial scaffold active against methicillin-and vancomycin-resistant Staphylococcus aureus." European Journal of Medicinal Chemistry **234**: 114204.

Hammad, A., N. S. Abutaleb, M. M. Elsebaei, A. B. Norvil, M. Alswah, A. O. Ali, J. A. Abdel-Aleem, A. Alattar, S. A. Bayoumi and H. Gowher (2019). "From phenylthiazoles to phenylpyrazoles: broadening the antibacterial spectrum toward carbapenem-resistant bacteria." Journal of medicinal chemistry **62**(17): 7998-8010.

Helal, A., A. Hussien, M. Elsebaei and A. Mayhoub (2022). "DESIGN AND SYNTHESIS OF NOVEL TERREMIDE AND SULFONAIDES DERIVATIVES FOR PHARMACOLOGICAL EVALUATION." Al-Azhar Journal of Pharmaceutical Sciences **66**(2): 126-137.

Helal, A. M., A. M. Sayed, M. Omara, M. M. Elsebaei and A. S. Mayhoub (2019). "Peptidoglycan pathways: there are still more!" RSC advances **9**(48): 28171-28185.

Herrmann, L., F. Hahn, C. Wangen, M. Marschall and S. B. Tsogoeva (2022). "Anti-SARS-CoV-2 Inhibitory Profile of New Quinoline Compounds in Cell Culture-Based Infection Models." Chemistry–A European Journal **28**(4): e202103861.

Hosny, Y., N. S. Abutaleb, M. Omara, M. Alhashimi, M. M. Elsebaei, H. S. Elzahabi, M. N. Seleem and A. S. Mayhoub (2020). "Modifying the lipophilic part of phenylthiazole antibiotics to control their drug-likeness." European journal of medicinal chemistry **185**: 111830.

Hwang, J. Y., T. Kawasuji, D. J. Lowes, J. A. Clark, M. C. Connelly, F. Zhu, W. A. Guiguemde, M. S. Sigal, E. B. Wilson and J. L. DeRisi (2011). "Synthesis and evaluation of 7-substituted 4-aminoquinoline analogues for antimalarial activity." Journal of medicinal chemistry **54**(20): 7084-7093.

Jia, C. Y., J. Y. Li, G. F. Hao and G. F. Yang (2020). "A drug-likeness toolbox facilitates ADMET study in drug discovery." Drug Discov Today **25**(1): 248-258.

Kozlov, M. (2022). "Why scientists are racing to develop more COVID antivirals." Nature **601**(7894): 496.

Kucharski, D. J., M. K. Jaszczak and P. J. Boratyński (2022). "A Review of Modifications of Quinoline Antimalarials: Mefloquine and (hydroxy)Chloroquine." Molecules **27**(3): 1003.

Mancy, A., N. S. Abutaleb, M. M. Elsebaei, A. Y. Saad, A. Kotb, A. O. Ali, J. A. Abdel-Aleem, H. Mohammad, M. N. Seleem and A. S. Mayhoub (2019). "Balancing physicochemical properties of phenylthiazole compounds with antibacterial potency by modifying the lipophilic side chain." ACS infectious diseases **6**(1): 80-90.

O'Donovan, D. H., C. De Fusco, L. Kuhnke and A. Reichel (2023). "Trends in molecular properties, bioavailability, and permeability across the bayer compound collection: miniperspective." Journal of medicinal chemistry **66**(4): 2347-2360.

Omara, M., M. Hagras, M. M. Elsebaie, N. S. Abutaleb, H. T. N. El-Din, M. O. Mekhail, A. S. Attia, M. N. Seleem, M. T. Sarg and A. S. Mayhoub (2023). "Exploring novel aryl/heteroaryl-isosteres of phenylthiazole against multidrug-resistant bacteria." RSC advances **13**(29): 19695-19709.

Sayed, A. M., N. S. Abutaleb, A. Kotb, H. G. Ezzat, M. N. Seleem, A. S. Mayhoub and M. M. Elsebaie (2023). "Arylpyrazole as selective anti-enterococci; synthesis and biological evaluation of novel derivatives for their antimicrobial efficacy." Journal of Heterocyclic Chemistry **60**(1): 134-144.

Schrezenmeier, E. and T. Dörner (2020). "Mechanisms of action of hydroxychloroquine and chloroquine: implications for rheumatology." Nature Reviews Rheumatology **16**(3): 155-166.

Shahin, I. G., K. O. Mohamed, A. T. Taher, M. M. Elsebaei, A. S. Mayhoub, A. E. Kassab and A. Elshewy (2023). "New Phenylthiazoles: Design, Synthesis, and Biological Evaluation as Antibacterial, Antifungal, and Anti-COVID-19 Candidates." Chemistry & Biodiversity **20**(11): e202301143.

Sharma, S., A. Deep, M. Malhotra and B. Narasimhan (2017). "Development of Antimalarial Drug Analogs to Combat Plasmodium Resistance." Handbook of Research on Medicinal Chemistry: 293-338.

Wang, C., P. W. Horby, F. G. Hayden and G. F. Gao (2020). "A novel coronavirus outbreak of global health concern." The lancet **395**(10223): 470-473.

Wang, Y., Y. Wang, Y. Chen and Q. Qin (2020). "Unique epidemiological and clinical features of the emerging 2019 novel coronavirus pneumonia (COVID-19) implicate special control measures." Journal of medical virology **92**(6): 568-576.

Wyman, K. A., A. S. Girgis, P. S. Surapaneni, J. M. Moore, N. M. Abo Shama, S. H. Mahmoud, A. Mostafa, R. F. Barghash, Z. Juan and R. D. Dobaria (2022). "Synthesis of potential antiviral agents for SARS-CoV-2 using molecular hybridization approach." Molecules **27**(18): 5923.

تشييد مشتقات جديدة للكلوروكين لدراستها بيولوجيا

عبد الله يوسف¹، عبد الرحمن صلاح ميهوب¹، قرنى عبد الله²، محمد مصطفى السباعي¹.

¹قسم الكيمياء العضوية – كلية الصيدلة (بنين) – جامعة الأزهر ـ القاهرة ـ مصر

²قسم الكيمياء العضوية التطبيقية، المركز القومى للبحوث، الجيزة ـ مصر

تُركِّز هذه الدراسة على تطوير مشتقات جديدة من الكلوروكين كعوامل مضادة للفيروسات المحتملة ضد فيروس كورونا المستجد (SARS-CoV-2). من خلال تعديل الموضع ٧ من الكلوروكين باستخدام تفاعلات اقتران، تم تركيب سلسلة من المركبات. حددت التقييمات المختبرية العديد من المشتقات ذات النشاط المضاد للفيروسات الواعدة، حيث أظهر المركب 9d تأثيرات مثبطة قوية ومؤشر انتقائي مناسب. تشير هذه النتائج إلى أن المشتقات توفر أساسًا واعدًا لمزيد من التحسين والتطوير كأدوية مضادة للفيروسات. يسلط هذا العمل الضوء على إمكانية التعديلات الهيكلية لتحسين فعالية مشتقات الكلوروكين. بالنظر إلى التحديات المستمرة لـ COVID-19، تستحق هذه المركبات الجديدة مزيدًا من البحث لتحديد آليات عملها وقيمتها العلاجية. توفر هذه الدراسة رؤية مهمة حول تطوير الأدوية المضادة للفيروسات وتسلط الضوء على الحاجة إلى الجهود المستمرة لتحسين الهياكل الدوائية الحالية في مكافحة التهديدات الفيروسية الناشئة.

الكلمات المفتاحية: الكلوروكين، مضاد الفيروسات، COVID-19 و تفاعلات الاقتران.